Vol. 38, No. 1
March 2020

JOURNAL OF
RADIATION
EFFECTS
Research and Engineering

Targeted Heavy-Ion Radiation of Aluminum Gallium Nitride/Gallium Nitride HEMTs

M.E. Mace, J.W. McClory, J.C. Petrosky, E. Heller, and G. Vizkelethy

This paper was presented at the 36th Annual HEART Conference
San Diego, CA, April 8–12, 2019.

Prepared by Amentum for the HEART Society under contract to NSWC Crane

This work was sponsored by the National Nuclear Security Administration (DE-NA000-3287). Views expressed in this paper are those of the authors and do not necessarily reflect the official policy or position of the Air Force, the Department of Defense, or the United States Government.

JOURNAL OF RADIATION EFFECTS,
Research and Engineering
Vol. 38, No. 1, March 2020

TARGETED HEAVY-ION RADIATION OF ALUMINUM GALLIUM NITRIDE/GALLIUM NITRIDE HEMTS

M.E. Mace, J.W. McClory, and J.C. Petrosky
Air Force Institute of Technology
Wright-Patterson Air Force Base, OH

E. Heller
Air Force Research Laboratory
Wright-Patterson Air Force Base, OH

G. Vizkelethy
Sandia National Laboratories[1]
Albuquerque, NM

Abstract

Ten aluminum gallium nitride (AlGaN)/gallium nitride (GaN) high-electron mobility transistors (HEMTs) were irradiated with 1.7 MeV germanium (Ge) ions using the Micrometer Resolution Optical, Nuclear, and Electron Microscope (Micro-ONE) system on the high-voltage engineering (HVE) 6 MV tandem accelerator at Sandia National Laboratories. Using the Micro-ONE system enabled targeting of the gate-drain gap of the transistors with the ions. In situ measurements captured degradation in the on and semi-on bias conditions after varying levels of ion fluence targeted in the gap region; no change to the off-bias condition was observed during in situ measurement. Pre- and post-irradiation output and transfer performance measurements—including threshold voltage, transconductance, drain current, and gate diode characteristics—were compared and analyzed. Changes to these performance characteristics in the on, off, and semi-on bias conditions included decreased transconductance, decreased drain current, and changes to the diode characteristics, but with no change to the threshold voltage. A delayed response between the start of the ion irradiation and an increased degradation in gate current was observed for both the on and semi-on-state bias. A delayed response between the start of ion irradiation and an increased degradation in drain current was also observed for the semi-on-state bias. Immediate degradation to the drain current during irradiation was observed in the on-state bias. These observed changes to the AlGaN/GaN HEMT device characteristics during 1.7 MeV Ge ion irradiation are correlated to similar performance degradation mechanisms observed in previous AlGaN/GaN HEMT reliability studies.

Introduction

Aluminum gallium nitride (AlGaN)/gallium nitride (GaN) high-electron mobility transistors (HEMTs) are used for power and radio frequency (RF) applications. Understanding how radiation affects reliability in GaN HEMTs is necessary to gain confidence in the technology for deployment in high-reliability space and defense applications. Failure mechanisms within AlGaN/GaN HEMTs have been attributed to non-temperature-related phenomena, different than failure mechanisms observed in silicon or gallium arsenide transistors [1]. These mechanisms include hot carrier and trap generation, contact degradation, and the inverse piezoelectric effect [2]. Certain degradation mechanisms are theorized to have different effects on device operation in direct current (DC) stress measurements [3]. Operating condition has also been identified as a factor in performance when coupled with radiation [4], [5]. This work focused on using targeted ion radiation at the Sandia Ion Beam Laboratory to deposit energy in the two-dimensional electron gas (2DEG) under different operating conditions (on, off, semi-on) to determine if the response provides insight to reliability

1 Sandia National Laboratories is a multimission laboratory managed and operated by National Technology & Engineering Solutions of Sandia, LLC, a wholly owned subsidiary of Honeywell International Inc., for the U.S. Department of Energy's National Nuclear Security Administration under contract DE-NA0003525.

This work was sponsored by the National Nuclear Security Administration (DE-NA000-3287). Views expressed in this paper are those of the authors and do not necessarily reflect the official policy or position of the Air Force, the Department of Defense, or the United States Government.

failure mechanisms seen in AlGaN/GaN HEMTs during stress operations. Targeted ion-beam radiation was applied at the gate-drain gap, a device region known to be susceptible to degradation caused by stress leading to reliability problems in device operation.

Reliability and qualification for silicon (Si) and gallium arsenide (GaAs) semiconductor devices are accomplished through accelerated life tests. These tests are based on the Arrhenius relationship, relating temperature, and reaction rates. This methodology is appropriate for Si and GaAs because elevated temperature has been shown to be a dominate failure mechanism. For GaN, the wider band-gap allows a higher-temperature operating regime, letting other failure mechanisms dominate and making accelerated life-testing techniques inappropriate for GaN technology. GaN does not have a dominate failure mechanism that affects reliability; instead, it has a multitude of reliability failure mechanisms that make qualification of these parts for use in space and nuclear environments challenging. A refined qualification protocol for GaN, in areas including the radiation environment and the intrinsic reliability, is currently an area of interest and research.

AlGaN/GaN HEMTs rely on the interface between the AlGaN and GaN, which forms a 2DEG. The wide band-gap of GaN devices results in higher mobility, greater temperature resistance, and higher radiation tolerance than traditional GaAs devices. Hence, the performance of GaN HEMTs has great promise for power and RF applications. Failure mechanisms of GaN HEMTs have been linked to point defects, inverse piezoelectric effect from mechanical stress, pits and cracks, and charge traps, along with many others. Many failure mechanisms have been identified at or near the drain edge of the gate and in the region between the gate and the drain.

GaN technology has typically performed well in radiation environments (total ionizing dose, single-event upsets, protons, neutrons, etc.) compared to Si or GaAs technology [6]. Applied bias combined with proton radiation has revealed differing degradation mechanisms that have been attributed to the growth techniques [5]. This research was designed to determine if the GaN device is location and bias sensitive to radiation. The gap between the gate and the drain was irradiated while under bias in an off, on, and semi-on state. Performance characterization measurements pre and post irradiation were compared.

Experiment

The AlGaN/GaN HEMT devices were manufactured, packaged, and wirebonded as commercial-grade test parts and used for stress-testing research [7]. However, not all were used during the stress-testing research; a subset of the devices remaining were used for this experiment. These devices were manufactured with technologies including an off center 0.5-µm t-gate, GaN cap, a gate-integrated field plate, source-connected field plate, and silicon nitride (SiN) passivation (grown by plasma-enhanced chemical vapor deposition), making the design relevant despite the device age. The HEMTs had two gates with a common drain and both gate widths were 50 µm. The gates contained a nickel Schottky barrier with thick gold overlay for low-gate resistance. The GaN buffer was grown by organometallic vapor phase epitaxy, the AlGaN barrier was undoped, and the substrate was silicon carbide (SiC) [7].

For this experiment, a custom circuit board was manufactured that allowed the packaged devices to be controlled by the Keysight Aligent 2902b two-channel source measurement unit (SMU) and the Quick IV Windows-based software as shown in Fig. 1. During all measurements, the source was common ground, and the gate and drain voltage were varied. All measurements were taken at room temperature. Pre-irradiation electrical characterization of the devices was accomplished to verify functionality and determine a comparison baseline.

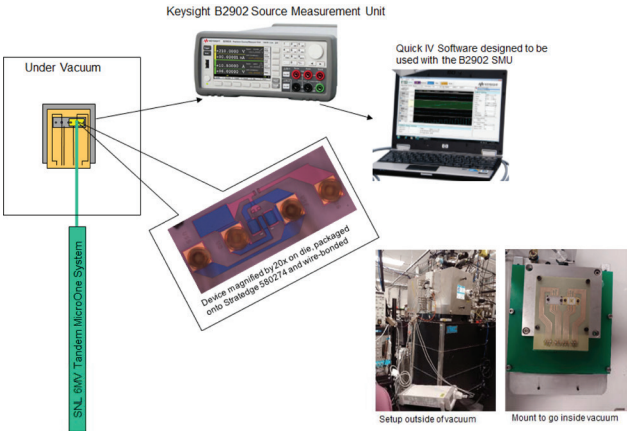

Figure 1. The experimental setup. The ion beam was directed at the specific location of the device and was measured using a B2902 SMU controlled by the computer program Quick IV.

In situ irradiation and post-irradiation electrical measurements were also collected.

The devices used had two gates with a common drain and separate sources for each gate built in a horizontal plane as shown in Fig. 2. During the irradiations, only one gate region was targeted. When the device was degraded via focused radiation to the point where one of the two gates failed (one finger of the device was irradiated to failure), the combined current reduced to approximately half of the original value, which is consistent with one gate being irradiated to failure while the other gate was functional. Because only one gate was irradiated, the second gate acted like a built-in control when accomplishing DC measurements. While not a true control because the non-irradiated gate region was not independently measurable, it did allow for irradiated devices to be measured even after one gate region was damaged to failure. This is different from broad-beam irradiation experiments where the beam irradiates the entire device and both gates of a 2×50 µm device would be irradiated equally.

Pre- and post-irradiation measurements consisted of transfer curve and output current-voltage (I-V) comparisons. The transfer curve held drain voltage at 0.1V, 0V, 1V, 5V, 10V, 15V, and 20V, and the gate voltage was swept from -4V to 1.3V in steps of 0.1V; gate and drain currents were measured. The output curve held the gate voltage 1V, 0V, -1V, -2V, -3V, -4V, and -5V, and the drain voltage was swept from 0V to 20V in steps of 0.2V; gate and drain currents were measured. *In situ* measurements applied bias in the off, on, and semi-on state. A constant voltage was held on the part before, during, and after irradiation, and the change to the gate and drain currents were measured. The off-state bias condition held the drain at 5V and the gate at -5V. The on-state bias condition held the drain at 5V and the gate at 1V. The semi-on-state bias condition held the drain at 5V and the gate at -2V. The average threshold voltage for these parts was measured during pre-irradiation measurements to be -3.1V.

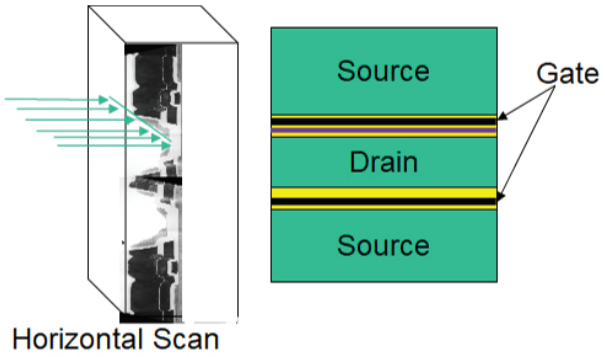

Figure 2. The horizontal scan of ions was accomplished by aiming the ion beam at the target and scanning the length of the device. The purple line on bottom correlates to the green arrows on the left targeting the gate-drain gap.

Stopping Range of Ions in Matter (SRIM) and Transport Range of Ions in Matter (TRIM) calculations were used to determine the type and energy of ions to maximize energy deposition in the targeted region [8]. The gate-drain gap experiment input into TRIM for the transport calculations is shown in Fig. 3. The ions were simulated to

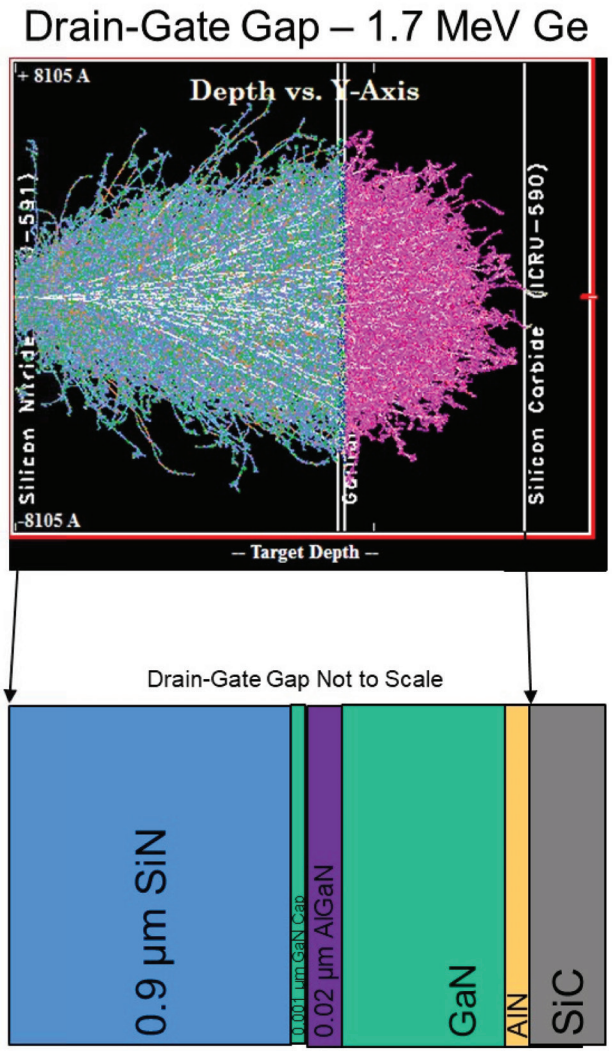

Figure 3. TRIM outputs of gate-drain gap simulation. The top-left chart show the Depth vs. Y axis spread of the Ge ions through the material stack shown on the bottom.

impact perpendicularly to the surface. Multiple ions and energies were run through the simulation to determine which ion and energy combination deposited the most energy at the interface. The 1.7 MeV germanium (Ge)-ion provided the best ion range when targeted through the gate-drain gap material as shown in the top-right of the quad of Fig. 4. The simulation showed that at the 2DEG, the amount of energy loss from recoils was approximately twice that from ionization as shown in the top-left of the quad of Fig. 4. The distribution of the type of ion being recoiled is shown in Fig. 5 (see next page). The energy loss due to recoils caused by the 1.7 MeV Ge ions will create an environment in the device that should result in observable effects of displacement damage at the 2DEG between the gate and the drain.

The Micrometer Resolution Optical, Nuclear, and Electron Microscope (Micro-ONE) system on the high-voltage engineering (HVE) 6 MV tandem accelerator at Sandia National Laboratory Ion Beam Laboratory was used to perform multiple 50-µm line scans along one finger at the gate-drain gap location of a 2×50 micrometer AlGaN/GaN HEMT device as shown in Figs. 6 and 7 (see next page). By only irradiating one gate-drain gap, the secondary gate-drain gap was undamaged; when irradiation damaged the first gate-drain gap region to the point where current did not flow, post-measurements were still possible through the secondary gate. Ten devices were irradiated with an average ion current of 1850±43 ions per second in the drain-gate gap location using 1.7 MeV Ge

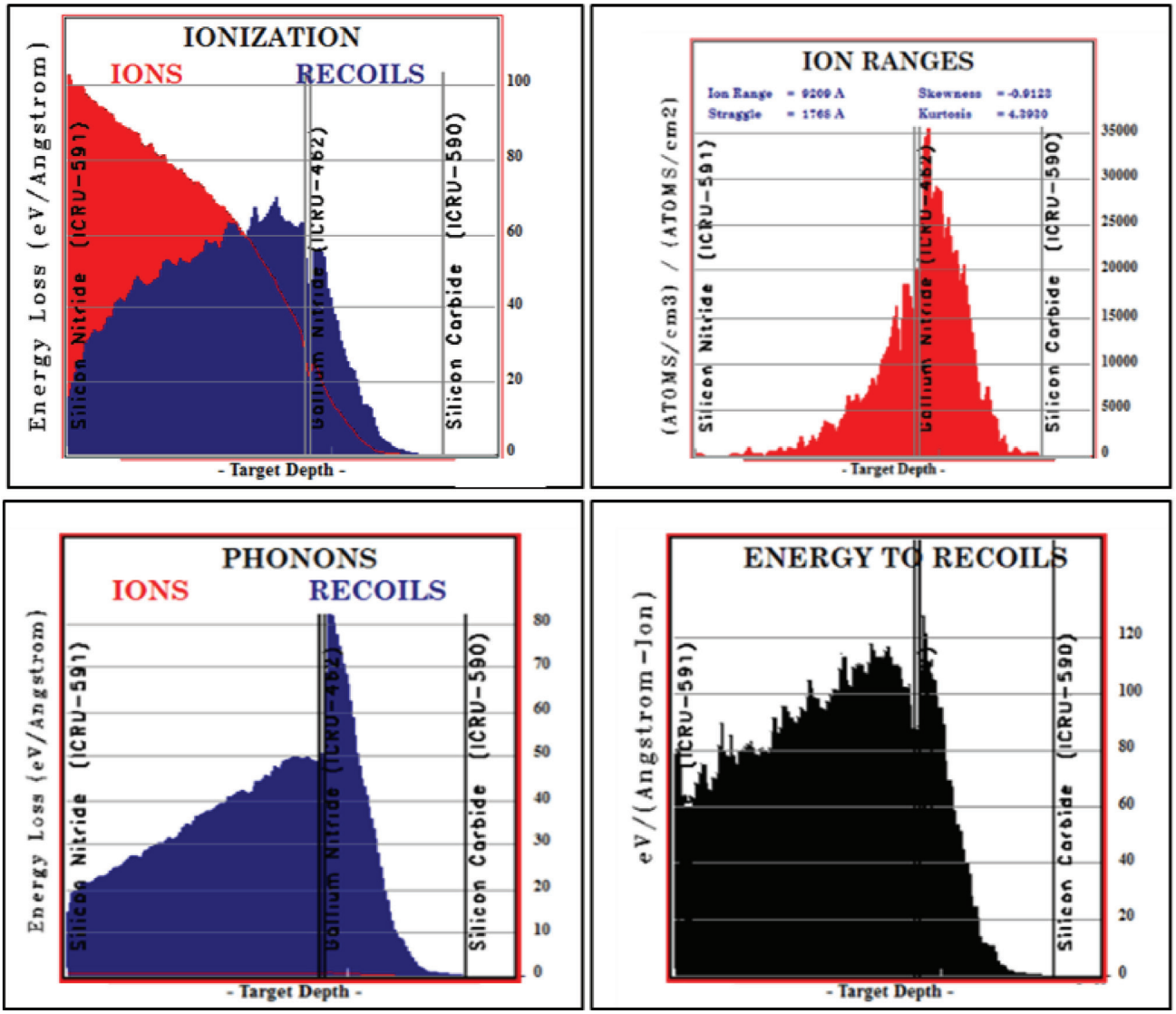

Figure 4. The quad charts show various TRIM output charts: Ionization vs. Recoils, Ion Range, Phonons, and Energy to Recoils.

ions. The ion current ranged from 1100–2900 ions/s during irradiation. Three devices were irradiated in the on state, three devices were irradiated in the off state, and four devices were irradiated in the semi-on state.

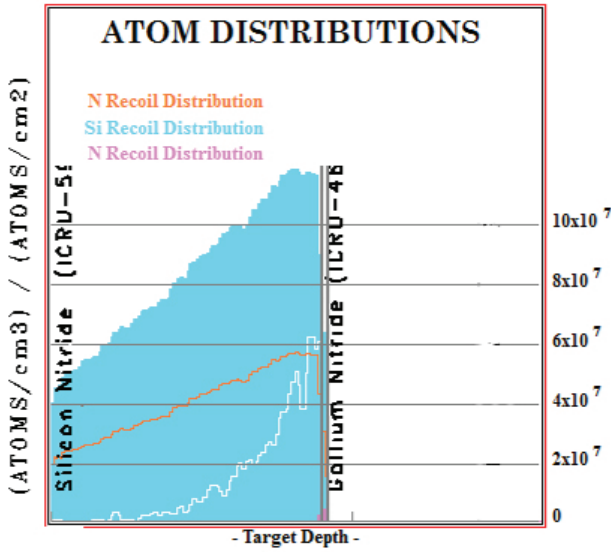

Figure 5. TRIM of the 1.7 MeV Ge ion through the gate-drain gap ion recoil distribution.

Figure 6. The target of the gate-drain gap irradiation.

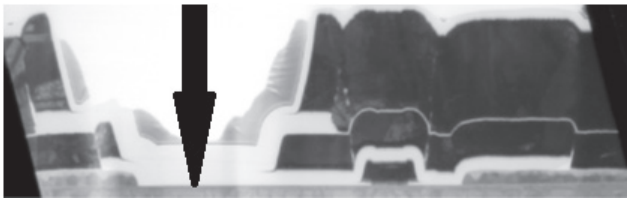

Figure 7. Transmission electron microscope cross section showing gate-drain gap target.

Results

The devices were irradiated while held at a constant drain and gate voltage. A horizontal 50-µm line scan, as described in Fig. 2, was rastered over the same line multiple times to increase fluence. The gap between one of the gates and the drain was targeted visually. The on-state and semi-on-state *in situ* irradiation is shown in Figs. 8 and 9, which capture a representative example of the

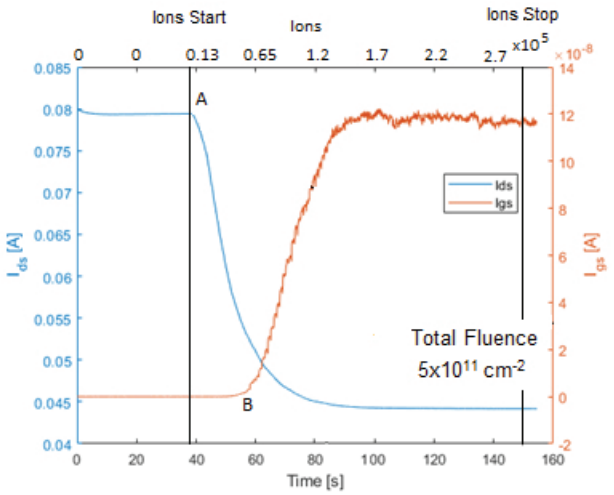

Figure 8. On-bias state during irradiation. Location A shows the drain current immediately decreased under irradiation, whereas location B shows that changes in gate current were delayed until the number of ions was approximately 5×10^4, which is a fluence of 1×10^{11} cm^{-2}. The total fluence received after the ions stopped was 5×10^{11} cm^{-2}.

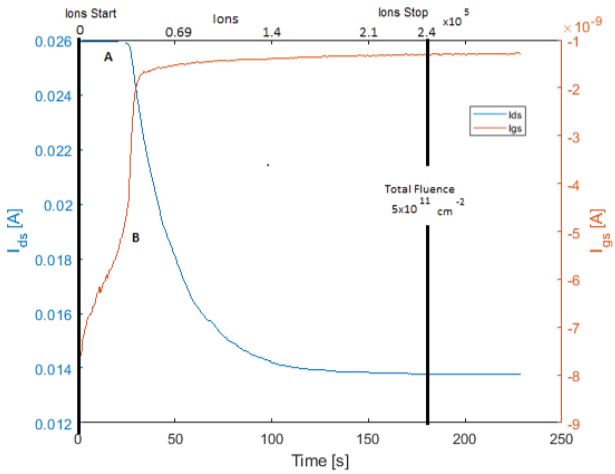

Figure 9. Semi-on state during irradiation. Location A shows that the drain current does not immediately decrease due to the ion strikes in the semi-on state. (It takes approximately 5×10^4 ions.) Location B shows that the gate current does not immediately increase due to the ion strikes in the semi-on state. (It takes approximately 5×10^4 ions.) The onset of significant changes in the drain (location A) and gate currents (location B) occurred at a fluence of 1×10^{11} cm^{-2}.

real-time drain current and gate current degradation associated with 1.7 MeV Ge ion irradiation while under bias. While in the off state, the drain and gate currents were insensitive to *in situ* degradation during irradiation as shown in Fig. 10. The black lines on Figs. 8, 9, and 10 indicate when the ions were started and when they were stopped in relation to when the device began measuring at the constant bias. The ion start times are different because the measurement was not automated. When the ions interacted with an on-state device, the drain current immediately started to decrease; however, the gate-leakage current did not immediately increase. In the semi-on bias state, the drain and gate currents both had a delay between when the Ge ions interacted with the device and degradation began. Both the drain current and gate current degraded in the on and semi-on state as shown in Figs. 8 and 9. The semi-on-state irradiation and constant bias began at the same time, which did not allow the device time to stabilize; the start of the ions was delayed to allow stabilization in subsequent bias states. However, even though the device was not stable at the time the ions started in Fig. 9, the rate of change of the gate current became steeper after ions were deposited, indicating a gate-leakage current degradation. Note the gate current becomes more positive in the on state and less negative in the semi-on state when it degrades.

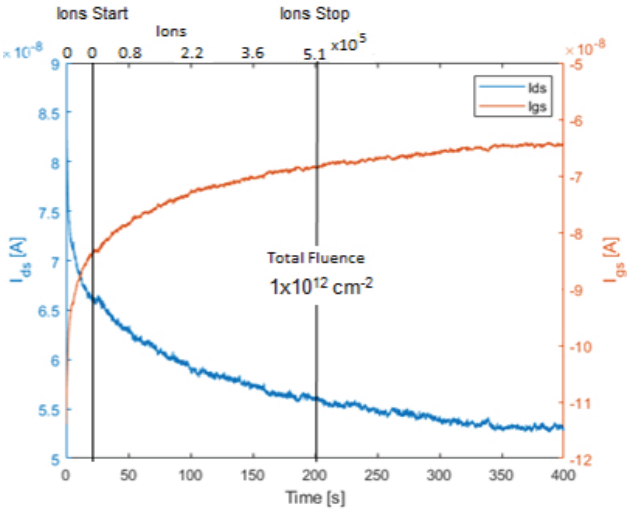

Figure 10. Off state during irradiation. No significant changes to drain or gate current was noted during irradiation. Note that the scale of the y-axes is 10^{-8}A for both drain and gate current in the off state.

When a delayed response in degradation was present during the *in situ* measurement, it occurred after an average of 5×10^4 Ge ions were deposited in the line scan across the 50-µm gate with a beam width of 1 µm (fluence of 1×10^{11} cm^{-2}). In all bias conditions tested, when the pre- and post-irradiation output and transfer measurements were compared, the post-irradiation measurements showed drain current degradation, transconductance degradation, and changes to the Schottky-gate-diode behavior when the drain voltages were 5V or higher. Threshold voltage was not affected because the depletion region under the gate was not targeted. The degradation varied depending on the fluence to which the device was exposed. All three bias states were found to degrade similarly based on fluence in post-irradiation performance measurements.

Analysis

The electric-field-induced gate-leakage current can cause the inverse piezoelectric effect that turns mechanical strain into lattice damage after a critical voltage is applied to the gate during step stress experiments. This damage is usually at the drain edge of the gate [9]. Additional phenomena associated with gate-leakage current degradation during stress tests include time-dependent gate degradation forming conductive percolative paths between the gate and channel and electrochemical gate degradation caused by oxidation at the drain edge of the gate [10]. Permanent damage from stress testing has been found to be caused by erosion and cracks in the epitaxial regions [11]. Displacement damage from Ge ions can also cause lattice damage. A study conducted by B.D. Weaver *et al.* mapped the calculated displacement damage dose in the drain current for different ion species and found the onset of degradation occurred after 1×10^{11} MeV/g [12]. A delayed response to irradiation was observed in the on and semi-on gate current and in the semi-on drain current, which shows that irradiation damage is bias dependent. A similar phenomenon was observed during stress testing by Joh and Del Alamo in which they found the V_{DGcrit} was bias dependent and attributed this to the impact of the strain field produced from the source side of the device [13]. A critical fluence causes the gate current to degrade at a certain value and causes the drain current to degrade differently based on bias. Both of these phenomena have been linked with a

critical voltage [13]. More research is needed to solidify the link between critical voltage and critical fluence to determine how radiation can be used as a tool to benefit the reliability community.

The ion damage was cumulative as shown in Fig. 11. One device was irradiated in the semi-on state targeting the metal contact over the gate and the gate-drain gap multiple times. First, the gate metal was targeted. After three irradiations, a total fluence of 2×10^{12} cm^{-2} was deposited in the gate metal. Post-irradiation performance characteristics were not substantially affected because the 1.7 MeV Ge ions did not have enough energy to penetrate to the semiconductor active region. The pre- and post-irradiation transconductance measurements associated with Fig. 11 are shown in Fig. 12.

Next, the gap between the gate and the drain was targeted. The first measurement of the gate-drain gap location is indicated by the solid blue line in Fig. 11 and the circle lines for the drain current and transconductance in Fig. 12. The delayed response observed in Fig. 9 was also observed in Fig. 11. When the ions were removed, the drain current flattened and did not continue to degrade. The gate current shown in Fig. 13 degraded only during the first gate-drain gap irradiation (corresponding to the solid blue line in Fig. 11); the remaining gate-drain gap

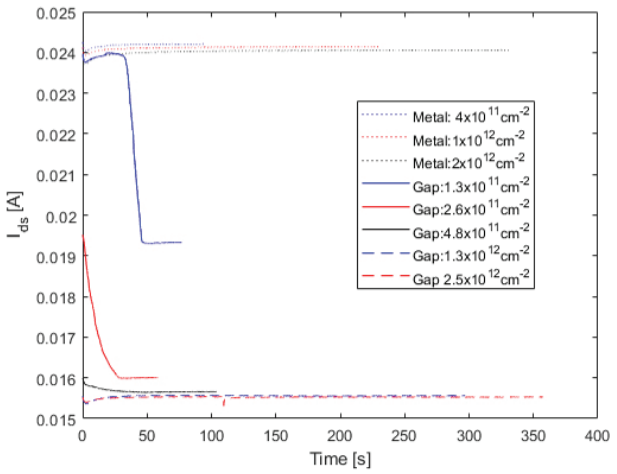

Figure 11. The effect of the radiation is cumulative. When 1.7 MeV Ge ions irradiated the metal over the gate/source area, little change was observed during the *in situ* measurement. Data from three irradiations in the metal were collected, and there was little change in the drain current after a cumulative fluence of 2×10^{12} cm^{-2} indicated by the final metal label. A delayed response was observed when the device was targeted in the gate-drain gap where the drain current decreased rapidly as shown by the blue line labeled "Gap": 1.3×10^{11} cm^{-2}. Each subsequent label in the legend labeled "Gap" indicates the cumulative fluence the gap location received at the end of another round of irradiation and measurements.

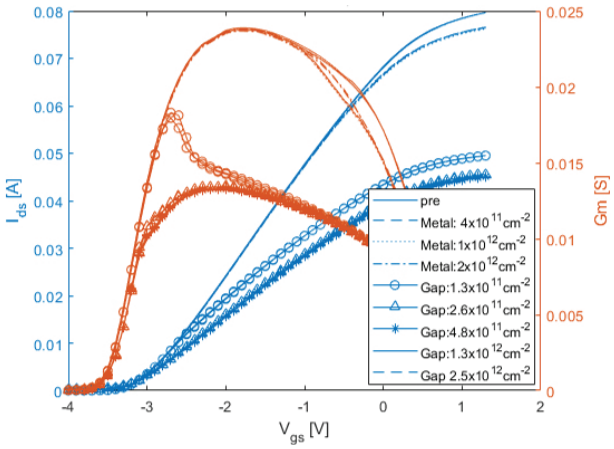

Figure 12. Transfer and transconductance curves post-irradiation of the irradiation shown in Fig. 11. The transfer curves (blue) show little to no threshold voltage shift, and the transconductance curves (red) show a decrease. The circle line for both the transfer and transconductance curve corresponds to the blue line in Fig. 11 (Gap: 1.3×10^{11} cm^{-2}).

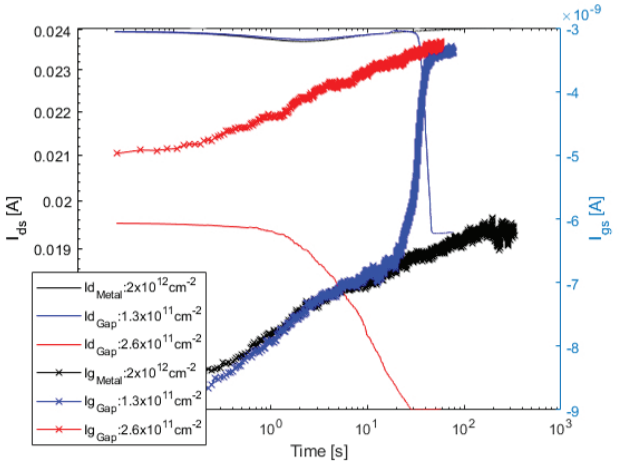

Figure 13. A semi-log representation of time along the x-axis showing the gate and drain current degradation. The black lines are for 1.7 MeV Ge ions targeted at the gold metal above the gate. The blue line indicates the first time the gate-drain gap is irradiated with multiple line scans depositing 1.3 MeV Ge ions/cm^{-2} in this specific location. The red indicates the second time the gate-drain gap is irradiated with multiple line scans causing an additional 1.3 MeV Ge ions/cm^{-2} fluence to interact, making the cumulative damage in the area 2.6 MeV Ge ions/cm^{-2}. Solid lines indicate the drain current that follows the left axis, and the x lines indicate the gate current that follows the right axis.

irradiations did not show a change in the gate current. The irradiation in a semi-on state was repeated, and the fluence values shown in the legends of Figs. 11 and 12 are cumulative.

The second gate-drain gap irradiation did not have a visible offset between ion impact and the drain current degradation. Additionally, the drain current did not recover and started to degrade at the same current level as the end of the previous irradiation. This is an indication of displacement damage. *In situ* measurements in the semi-on state were repeated until the finger of the device was no longer functioning, noted by the drain current reduction by approximately 50%, reaffirming that the radiation is only interacting with one of the two gates. The transconductance after the gate-drain gap was irradiated the first time with a cumulative damage of 1.3×10^{11} cm^{-2} was irregular for drain voltages of 5V and greater during the measurements as shown in Fig. 12. This was likely caused by the non-linearity of the drain resistance compared to the source resistance and is more noticeable for the higher drain-voltage measurements [14]. The resistance was likely increased due to the displacement damage in and around the 2DEG created by the Ge ions and the subsequent recoils that occurred in the lattice atoms between the gate and the drain, increasing scattering and thus reducing the mobility. This is a similar effect that has been observed in stress testing causing an inverse piezoelectric effect from mechanical strain causing defect damage to the lattice.

The transfer curve measurements (i.e., varying the gate voltage with a constant drain voltage) were recorded first during the post-irradiation measurement; both the on-state or semi-on-state devices responded as expected. However, when the output curve measurements were initiated (i.e., varying the drain current with a constant gate voltage), some of the on-state and semi-on-state devices responded with large gate currents. When output data was measured for the on-state devices, one of the three devices burned out, as shown in Fig. 14. When the output data was measured for the semi-on-state devices, two of the four devices caused the measurement system to hit compliance and cease recording data. This could have been due to the drain voltage sweep (0–20V) interacting with the higher resistance region between the gate and the drain, causing the current to increase beyond the limit of the device; however, more research is required as to the exact cause of the unusual behavior.

Figure 14. Same part pre-irradiation (left) and post-irradiation (right). The burn mark (blackened area) appeared during post-irradiation in the on-state output measurements, when the gate voltage was held constant and the drain voltage was swept from 0 to 20V.

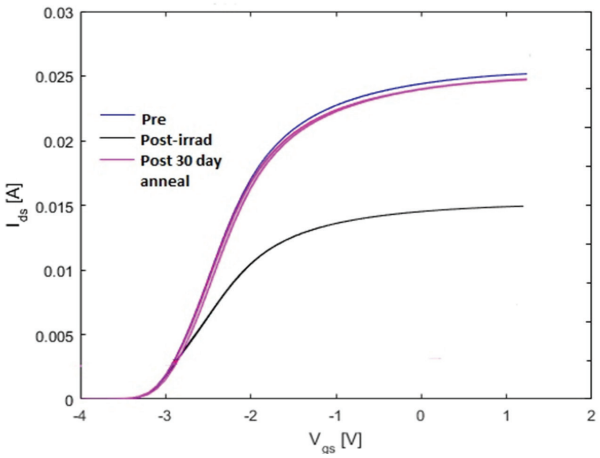

Figure 15. Pre-irradiation, post-irradiation, and post 30-day room-temperature, anneal-IV measurements compared. Drain voltage held constant at 1V during measurements.

Post-irradiation measurement of one semi-on device showed that the drain current recovered after a 30-day room-temperature anneal, as shown in Fig. 15. The gate diode characteristics were changed due to the irradiation and then almost fully recovered after the 30-day room-temperature anneal as well. The device that recovered had both delayed-drain and gate-current degradation; the drain current flattened in a similar manner to that observed in the first gate-drain gap irradiation (solid blue line) during the cumulative damage experiment as shown in Fig. 11. However, during the data collection of additional post-anneal measurements, this device failed to turn off. The other nine devices were irradiated until the

finger of the device was no longer functioning; therefore, the exact conditions necessary for recoverability from ion damage in the gate-drain gap are unknown.

Electrical stress and proton-irradiation-induced defects have been correlated by Jiang *et al.* [5], who also noted that an on-state bias may enhance different defects than those produced when an off-state bias was applied. Semi-on-state stress and proton irradiation have been correlated to cause the same defects [5]. More research is required to determine the cause of the offset of the drain current degradation in the semi-on state versus its immediate degradation in the on-state as identified in this research. It could be due to both the on-state bias and the Ge ion irradiation causing the same defect (V_N perhaps), thereby increasing the degradation associated with that defect immediately. Perhaps the semi-on bias and the Ge ion irradiation does not immediately create the same defect; instead, it takes time for the increased number of those defects to be created (V_{Ga}-V_N -H_x perhaps).

Conclusion

Irradiating through the drain-gate gap in the on, off, and semi-on bias conditions caused significant reduction in transconductance and changes to gate diode behavior at higher drain voltages. There were no changes in threshold voltage noted for on, off, or semi-on bias states. Increased gate current and decreased drain current was observed during the on state and semi-on states when measured *in situ* with 1.7 MeV Ge ion irradiation. In the semi-on state and on state, a fluence of 1×10^{11} cm^{-2} was a representative critical fluence observed to increase gate current. This same critical fluence was also observed to decrease drain current when irradiated in the semi-on state. However, in the on-state bias, the drain current degradation was immediately observed. The direct cause of the different behavior of the drain current degradation between the semi-on state and on-state bias when coupled with 1.7 MeV Ge ions targeted in the gap between the gate and the drain is unknown at this time. Overall, targeted irradiation along the gate-drain gap appears to replicate similar performance characteristic degradations observed in reliability studies of AlGaN/GaN HEMTs. Further research using this technique may help both the reliability and radiation effects communities to better understand failure mechanisms within AlGaN/GaN HEMTs.

Using a microbeam to target specific areas of semiconductor devices allowed degradation to be observed *in situ* under different operating conditions. The observed *in situ* degradation was correlated to changes in performance characteristics. No threshold voltage shift, for example, indicated that the active region under the gate was not affected in a targeted experiment of the gate-drain gap. The amount of degradation in performance characteristics can be correlated to the amount of radiation damage in a specific region when using this technique. Defects introduced in and near the 2DEG cause decreases in the 2DEG density and electron mobility, which decreases drain current. By using the microbeam to target specific areas of the device, degradation can be captured *in situ,* helping to pinpoint failure locations as well as validate modeling and simulation software designed to identify device reliability parameters. Improved qualification protocol for radiation and intrinsic reliability can also be informed by using this technique to understand failure limits due to defects and radiation damage.

Acknowledgment

The authors would like to thank the Ion Beam Laboratory staff at Sandia National Laboratories and B.A. Bozada, B.S. Poling, A.M. Hilton, and J.L. Brown from the Sensors and Materials Directorates of the Air Force Research Laboratory.

References

[1] J. Coutu *et al.*, "Benefits of considering more than temperature acceleration for GaN HEMT life testing," *Electron.*, vol. 5, no. 32, pp. 1–14, 2016.

[2] D.J. Cheney *et al.*, "Reliability studies of AlGaN/GaN high electron mobility transistors," *Semiconductor Sci. Technol.*, vol. 28, no. 074019, p. 12, 2013.

[3] B.M. Paine, S.R. Polmanter, V.T. Ng, N.T. Kubota, and C.R. Ignacio, "Lifetesting GaN HEMTs with multiple degradation mechanisms," *IEEE Trans. Device Materials Rel.*, vol. 15, no. 4, pp. 486–494, 2015.

[4] J. Chen *et al.*, "Effects of applied bias and high field stress on the radiation response of GaN/AlGaN HEMTs," *IEEE Trans. Nucl. Sci.*, vol. 62, no. 6, 2015.

[5] R. Jiang *et al.*, "Multiple defects cause degradation after high field stress in AlGaN/GaN HEMTs," *IEEE Trans. Nucl. Sci.*, vol. 18, no. 3, 2018.

[6] S.J. Pearton, F. Ren, E. Patrick, M.E. Law, and A.Y. Polyakov, "Review-ionizing radiation damage effects on GaN devices," *ECS J. Solid State Sci. Technol.*, vol. 5, no. 2, pp. Q35–Q60, 2016.

[7] B.D. Christiansen, E.R. Heller, R.A. Coutu, Jr., R. Vetury, and J.B. Shealy, "A very robust AlGaN/GaN technology to high forward gate bias and current," *Active Passive Electron. Components*, pp. 1–4, 2012.

[8] J.F. Ziegler, J.P. Biersack, and M.D. Ziegler, *SRIM: The Stopping and Range of Ions in Matter*, Morrisville, NC: Lulu Press Co., 2018.

[9] J.A. del Alamo and J. Joh, "GaN HEMT reliability," *Microelectron. Rel.*, vol. 49, no. 9, pp. 1200–1206, 2009.

[10] E. Zanoni, "GaN HEMT reliability research - A white paper," Department of Information Engineering, University of Padova, Veneto, Italy, Tech. Rep., 2017.

[11] E. Zanoni *et al.*, "A review of failure modes and mechanisms of GaN-based HEMTs," in *2007 IEEE Int. Electron Devices Meeting*, Dec. 2007, pp. 381–384.

[12] B. Weaver, P. Martin, J. Boos, and C. Cress, "Displacement damage effects in AlGaN/GaN high electron mobility transistors," *IEEE Trans. Nucl. Sci.*, vol. 59, no. 3077, 2010.

[13] J. Joh and J. del Alamo, "Critical voltage for electrical degradation of GaN high-electron mobility transistors," I*EEE Electron. Device Lett.*, vol. 29, no. 4, pp. 287–289, 2008.

[14] C.-H. Chen *et al.*, "The causes of GaN HEMT bell-shaped transconductance degradation," *Solid-State Electron.*, no. 126, pp. 115–124, 2016.